ChemComm
Chemical Communications

Accepted Manuscript

This article can be cited before page numbers have been issued, to do this please use: S. S. Roy, W. Iali, G. A. I. Moustafa and M. H. Levitt, *Chem. Commun.*, 2022, DOI: 10.1039/D1CC06973J.

ROYAL SOCIETY OF CHEMISTRY

rsc.li/chemcomm

View Article Online
DOI: 10.1039/D1CC06973J

COMMUNICATION

Tuning of pH Enables Carbon-13 Hyperpolarization of Oxalates by SABRE

Received 00th January 20xx,
Accepted 00th January 20xx

DOI: 10.1039/x0xx00000x

Soumya S. Roy,[a,b*] Wissam Iali,[c,d*] Gamal A. I. Moustafa [a] and Malcolm H. Levitt [a]

Nuclear spin hyperpolarization transforms typically weak NMR responses into strong signals paving the way for low-gamma nuclei detection within practical time-frames. SABRE (Signal Amplification by Reversible Exchange) is a particularly popular hyperpolarization technique due to its simplicity but the pool of molecules it can polarize is limited. The recent advancement in the form of co-ligands has made SABRE applicable towards molecules with O-donor sites e.g. pyruvate, a key step towards its potential clinical application. Here we explore the SABRE hyperpolarization of another compound with an alpha-keto motif, namely oxalate. We show that hyperpolarization of oxalate may be achieved by adjusting the pH in the presence of sulfoxide co-ligands. The SABRE effect for oxalate in methanol solutions is most effective for the mono-protonated form, which is dominant in the solution around pH ~ 2.8. The polarization levels become markedly lower at both higher and lower pH. Employing 50% enriched pH_2 we achieve up to 0.33% net ^{13}C polarization in mono-protonated oxalate. In an alternate procedure we show that the hyperpolarization effect in oxalates can also be realised by synthesizing an esterified version of it, without any substantive pH implications. Further, the procedures to create hyperpolarized singlet orders in such substrates are also investigated.

The inherently low nuclear spin polarization can be increased dramatically through the process of hyperpolarization, leading to increased sensitivity of target nuclei by several orders of magnitude. Among the few techniques available, Para Hydrogen Induced Polarization (PHIP) offers a cost-effective, fast and relatively simple routes to enhance NMR signals.[1] A variant of PHIP, known as SABRE (Signal Amplification by Reversible Exchange) is particularly popular due to its simplicity and reversible nature.[2, 3] SABRE does not require any chemical alteration in order to transfer polarization from highly ordered para-hydrogen (pH_2) to target nuclei of the substrate. Instead, the substrate and the pH_2 both bind transiently to a suitable metal catalyst to form polarization transfer pathways based on scalar-coupling networks.[4] When resonance matching conditions are met, transfer of polarization takes place in a fast and reversible fashion. Since its inception in 2009, SABRE has been used to hyperpolarize a large class of important substrates containing nuclei such as ^{1}H, ^{13}C, ^{15}N, ^{31}P and others.[5-8] However, the majority of these are molecules with an N-donor ligand.

Recently, this limitation has been elegantly alleviated using the relay mechanism in which exchangeable protons are employed to facilitate polarization transfer and hyperpolarization of molecules other than N-heterocycles.[9, 10] Also, using sulfoxides as co-ligands to the Ir-NHC catalyst has enabled SABRE to hyperpolarize weakly ligating O-donor substrates e.g. pyruvate and acetate (Scheme 1).[11, 12] The mechanistic studies of pyruvate revealed that the presence of DMSO as a co-ligand provides the required stabilization of the catalytic species in order to allow weakly binding O-donors to ligate to the iridium in a reversible fashion.[13] Oxalate also contain a similar α-keto acid moiety similar to pyruvate and may therefore be expected to behave in a similar fashion. However, when oxalate was tried, a chelated oxalate-iridium complex was

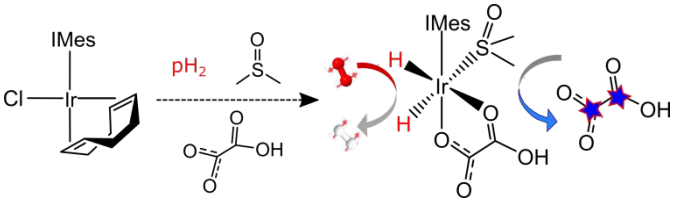

Scheme 1: Schematic of SABRE mechanism in the presence of dimethyl sulfoxide (DMSO) as a co-ligand. Oxalate binds to the Ir-IMes catalyst forming a transitory catalytic species to unlock the latent polarization of pH_2 and subsequent transfer of it via the iridium metal centre.

[a] School of Chemistry, University of Southampton, University Road, Southampton, SO17 1BJ, United Kingdom. E-mail: S.Roy@soton.ac.uk
[b] CBR Division, Defence Science and Technology Laboratory (Dstl), Porton Down, Salisbury, SP4 0JQ, United Kingdom.
[c] Department of Chemistry, King Fahd University of Petroleum & Minerals (KFUPM), Dhahran 31261, Saudi Arabia. E-mail: wissam.iali@kfupm.edu.sa
[d] Center for Refining & Advanced Chemicals, Dhahran 31261, Saudi Arabia.
[e] † Footnotes relating to the title and/or authors should appear here.
Electronic Supplementary Information (ESI) available: [details of any supplementary information available should be included here]. See DOI: 10.1039/x0xx00000x

formed that hindered the ligand exchange mechanism of SABRE.[13]

In this report we demonstrate a simple route to the hyperpolarization of oxalate by SABRE by tuning the pH level of the substrate in the presence of Ir-NHC catalyst and a sulfoxide co-ligand. A direct relationship between the polarization efficiency and the pH level is established. SABRE-SHEATH (SHield Enables Alignment Transfer to Heteronuclei)[14] conditions are optimized to achieve the maximum polarization levels. In addition, possible routes to achieve long-lasting singlet hyperpolarization are also discussed.

A series of disodium oxalate solutions was prepared with pH values between 0 and 6 by mixing of NaOH droplets into oxalic acid solutions in a step-wise fashion. In order to achieve the near zero pH level, H_2SO_4 was added instead (see ESI for more details). Figure 1 displays the molar fraction of three forms of oxalates with respect to the pH level of solutions in 5:1 methanol-water mixture.[15] At room temperature, the pK_a values of the oxalate solutions are experimentally measured as 1.27 and 4.27 respectively.

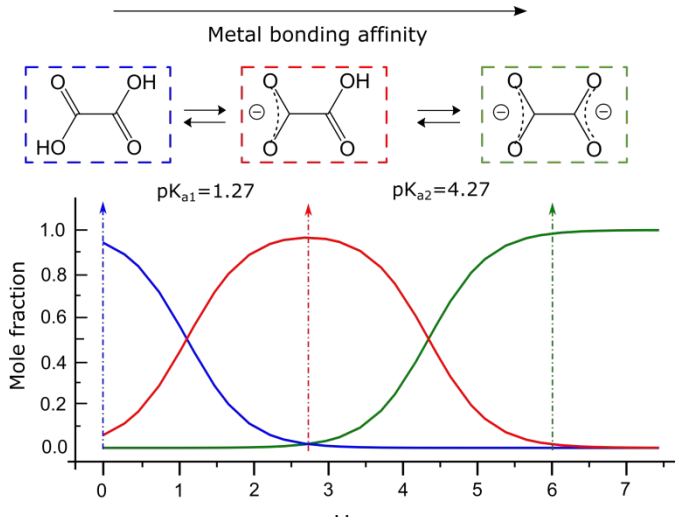

Figure 1: Three forms of oxalates based on protonation constant and their ratios depending on pH value. At around pH of 2.8, more than 90% of molar fraction of the solution consists of the mono-protonated oxalate form (Red curve) whilst lower and higher pH numbers represent acid (Blue curve) and basic (Green curve) form of oxalates respectively.

The established SABRE experimental protocol was followed. A J-Young's NMR tube containing 5 mM [IrCl(COD)IMes] catalyst and 20 mM DMSO-d_6 was first activated with 4 Bar H_2 in 0.5 ml methanol-d_4 solution. Due to the poor solubility in methanol, 0.1 ml of a 40 mM solution of oxalate in D_2O was prepared before mixing it into the methanol solution. After degassing the NMR samples by 3 cycles of freeze-pump-thaw method, 50% enriched pH_2 was added at 4 bar pressure. SABRE experiments were performed by shaking the tube inside a microtesla field (0.4 μT) for ~10 seconds and subsequently placing the NMR tube in a 9.4 T magnet for signal detection.[14, 16] A hard 90° pulse was applied to observe ^{13}C NMR signals from the SABRE solutions. The experiment with oxalate at pH = 0.0 does not show any observable ^{13}C NMR signal upon detection. However, when oxalate at pH = 1.8 was employed, a strong and single resonance ^{13}C NMR signal was detected at around 162 ppm. This hyperpolarized signal is readily assigned to the free oxalate since the bound species is expected to produce two chemically distinct signals based on observations made earlier.[13] An even stronger ^{13}C NMR signal was detected when SABRE was performed on an oxalate solution at pH = 2.8. The hyperpolarization effect gradually decreased with increasing pH until the signal became undetectable at pH = 6.0. Figure 2 shows the hyperpolarized ^{13}C signals of oxalate solutions as a function of pH and Table 1 summarises the data.

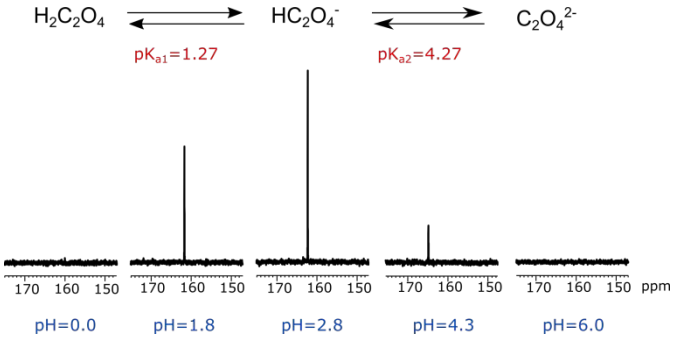

Figure 2: The effect of pH level on the hyperpolarized ^{13}C signal of oxalate. A maximum ^{13}C signal was achieved at a pH of 2.8 with a drop in enhancement at both higher and lower pH values.

Table 1: ^{13}C chemical shifts (δ), Enhancement factors (over thermal equilibrium signals at 9.4 T) and corresponding ^{13}C net polarization levels of oxalates with different pH values. No detectable ^{13}C NMR signals were observed for oxalates with pH=0 and 6.

pH values of oxalate	^{13}C chemical shift (δ/ppm)	^{13}C enhancement factors (ε)	Net ^{13}C polarization (%)
1.8	161.65	~305	~0.25%
2.8	162.27	~400	~0.33%
4.3	164.84	~130	~0.11%

These results may be explained by postulating that the binding of oxalate to a metal site depends strongly on pH, presumably since hydronium ions compete with the metal for attachment to the negatively charged oxygen atoms of the oxalate. Therefore, the oxalate-metal bonding affinity can be controlled by the pH level. The mono-protonated sodium oxalate (pH 2.8) provides the required stabilisation to facilitate effective reversible ligand exchange process of SABRE. The hyperpolarized signal is therefore roughly proportional to the concentration of the mono-protonated oxalate species in solution, which is greatest around pH = 2.8, and lower at both higher and lower pH. At lower pH, oxalate stays in the solution and does not bind to the catalyst. While, at high pH, oxalate binds strongly to the catalyst since a stable chelate can be formed between the stabilised carboxylate (COO^-) groups and

the iridium metal centre. In an intermediate pH level, the binding affinity of oxalate towards the catalyst is significantly reduced since one of the carboxylates is blocked by protonation and consequently a reversible binding of oxalate on the iridium metal centre become feasible (see ESI for characterization data). To establish the optimum SABRE-SHEATH condition,[14] a typical magnetic field profile study was carried out with maximum signal achiving at 0.4 μT mixing (See ESI). Figure 3 illustrates the result with a carbon-13 enhancement factor of ~400 is estimated at pH = 2.8 relative to a non hyperpolarized solution at 9.4 T (net ^{13}C polarization 0.33%).

An alternative route to reduce the binding affinity of oxalates with the metal centre can be realized by esterifying one of the carboxylate groups. To prove this concept, we synthesised ethyl-d_5-$^{13}C_2$-oxalate which is fully soluble in methanol and is readily polarized by SABRE. Figure 4 demonstrates the SABRE hyperpolarized spectra of this ester by following similar protocols as outlined above, confirming the fact that esterification does not hinder their SABRE affinity. The obtained ^{13}C enhancement factor for this oxalate ester was about 80-fold as compared to non-hyperpolarized sample at 9.4 T. This enhancement is significantly less than the oxalate solution at pH = 2.8, which may be attributed to the fact that the esterified oxalate is more sterically bulky than the oxalate and as a consequence might bind weaker to the catalyst or inhibit faster exchange to the Ir metal centre. In addition, the

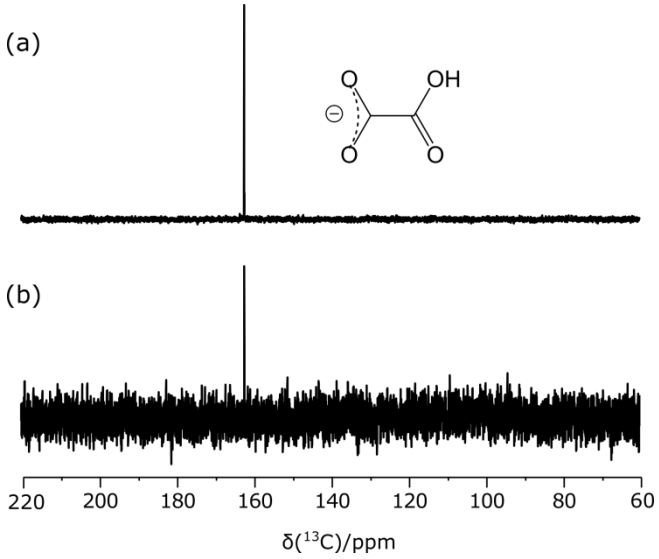

Figure 3: ^{13}C NMR spectra of oxalate at pH = 2.8 acquired by (a) 1 scan 90° pulse following SABRE hyperpolarization procedure and (b) corresponding thermal equilibrium signal averaged over 400 transients with a recycle delay of 200 s.

electronic configuration of the oxalate ester in combination with the catalyst can also impact negatively in determining the resulting signal enhancements after polarization transfer.[17, 18]

SABRE has been coupled with long-lived singlets (LLS) to generate long-lived hyperpolarized singlet order lasting over tens of minutes in particular substrates.[19-23] Attempts were made to use SABRE to hyperpolarize long-lived singlet order in the $^{13}C_2$ pairs of $^{13}C_2$-labelled oxalate (ESI, section S5). Disappointingly though, this system was found to be not

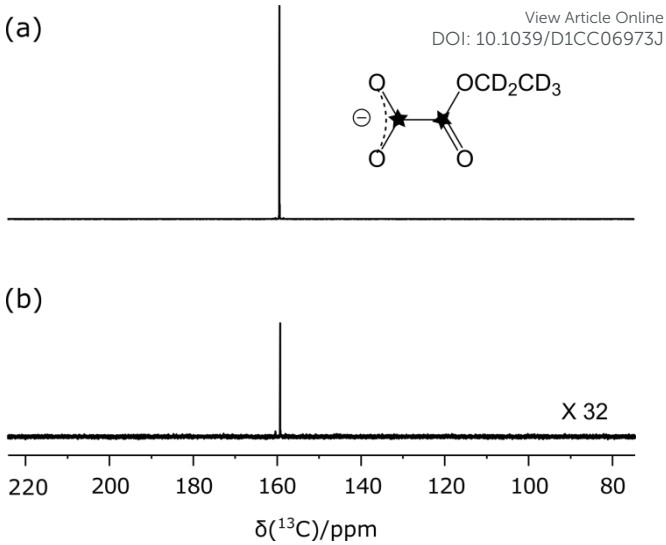

Figure 4: ^{13}C NMR spectra of ethyl-d_5-$^{13}C_2$-oxalate acquired by 1 scan 90° pulse following (a) SABRE hyperpolarization procedure (S/N: ~1200) and (b) corresponding thermal equilibrium signal of non-hyperpolarized solution (vertically scaled by 32 times).

suitable for supporting long singlet lifetimes. It is possible that the ^{13}C-pair singlet order in $^{13}C_2$-oxalate is relaxed by a chemical exchange mechanism, as is the case in the related system of $^{13}C_2$-labelled squarate.[24] The singlet results in conjunction with the hyperpolarization are summarized in the ESI.

In summary, two complimentary methods of generating hyperpolarized oxalate species by SABRE have been presented. In the first method the bonding affinity between oxalate and the SABRE catalyst is controlled by changing the pH level. A strong correlation of ^{13}C signal enhancement with the pH is observed. Using 50% enriched pH_2 at 4 Bar of pressure, we achieved up to 0.33% net ^{13}C polarization in the case of mono-protonated sodium oxalate at pH = 2.8. In the second procedure, mono-esterification is used to allow the oxalate to bind reversibly with the iridium catalyst and consequently facilitating the SABRE mechanism. Although, the achieved polarization is relatively low in this work, there is much room for optimization of the experimental factors e.g. pH_2 concentration, catalysts, temperature and pressure. Unfortunately, the preliminary results of long-lived singlet hyperpolarization in the case of an oxalate ester does not provide any additional benefit in terms of spin lifetime. However, a better understanding of relaxation mechanisms in such molecules might lead to a convenient route to create long-lasting hyperpolarization in oxalate and similar α-keto acid motifs with potential applications in metabolic imaging.

This work was supported by the EPSRC-UK (EP/P009980/1), the ERC (786707-FunMagResBeacons), and the University of Southampton. WI acknowledges support from the KFUMP-funded Grant-SR191019. We thank Weidong Gong for instrumental support.

Authors declare no conflict of interests.

Notes and references

1. J. Natterer and J. Bargon, *Prog. Nucl. Mag. Res. Sp.*, 1997, **31**, 293-315.
2. C. R. Bowers and D. P. Weitekamp, *Phys. Rev. Lett.*, 1986, **57**, 2645-2648.
3. R. Eisenberg, *Acc. Chem. Res.*, 1991, **24**, 110-116.
4. R. W. Adams, J. A. Aguilar, K. D. Atkinson, M. J. Cowley, P. I. P. Elliott, S. B. Duckett, G. G. R. Green, I. G. Khazal, J. Lopez-Serrano and D. C. Williamson, *Science*, 2009, **323**, 1708-1711.
5. H. Zeng, J. Xu, J. Gillen, M. T. McMahon, D. Artemov, J.-M. Tyburn, J. A. B. Lohman, R. E. Mewis, K. D. Atkinson, G. G. R. Green, S. B. Duckett and P. C. M. van Zijl, *J. Mag. Res.*, 2013, **237**, 73-78.
6. T. Theis, M. L. Truong, A. M. Coffey, R. V. Shchepin, K. W. Waddell, F. Shi, B. M. Goodson, W. S. Warren and E. Y. Chekmenev, *J. Am. Chem. Soc.*, 2015, **137**, 1404-1407.
7. N. Eshuis, B. J. A. van Weerdenburg, M. C. Feiters, F. P. J. T. Rutjes, S. S. Wijmenga and M. Tessari, *Angew. Chem. Int. Ed.*, 2015, **54**, 1481-1484.
8. R. E. Mewis, R. A. Green, M. C. R. Cockett, M. J. Cowley, S. B. Duckett, G. G. R. Green, R. O. John, P. J. Rayner and D. C. Williamson, *J. Phys. Chem. B*, 2015, **119**, 1416-1424.
9. S. S. Roy, K. M. Appleby, E. J. Fear and S. B. Duckett, *J. Phys. Chem. Lett.*, 2018, **9**, 1112-1117.
10. W. Iali, P. J. Rayner, A. Alshehri, A. J. Holmes, A. J. Ruddlesden and S. B. Duckett, *Chem. Sci.*, 2018, **9**, 3677-3684.
11. M. E. Gemeinhardt, M. N. Limbach, T. R. Gebhardt, C. W. Eriksson, S. L. Eriksson, J. R. Lindale, E. A. Goodson, W. S. Warren, E. Y. Chekmenev and B. M. Goodson, *Angew. Chem. Int. Ed.*, 2020, **59**, 418-423.
12. W. Iali, S. S. Roy, B. J. Tickner, F. Ahwal, A. J. Kennerley and S. B. Duckett, *Angew. Chem. Int. Ed.*, 2019, **58**, 10271-10275.
13. B. J. Tickner, J. S. Lewis, R. O. John, A. C. Whitwood and S. B. Duckett, *Dalton Trans.*, 2019, **48**, 15198-15206.
14. T. Theis, M. L. Truong, A. M. Coffey, R. V. Shchepin, K. W. Waddell, F. Shi, B. M. Goodson, W. S. Warren and E. Y. Chekmenev, *J. Am. Chem. Soc.*, 2015, **137**, 1404-1407.
15. X. Xue, W. Wang, H. Fan, Z. Xu, I. Pedruzzi, P. Li and J. Yu, *Adsorption*, 2019, **25**, 1191-1204.
16. M. L. Truong, T. Theis, A. M. Coffey, R. V. Shchepin, K. W. Waddell, F. Shi, B. M. Goodson, W. S. Warren and E. Y. Chekmenev, *J. Phys. Chem. C*, 2015, **119**, 8786-8797.
17. P. J. Rayner, M. J. Burns, A. M. Olaru, P. Norcott, M. Fekete, G. G. R. Green, L. A. R. Highton, R. E. Mewis and S. B. Duckett, *Proc. Natl. Acad. Sci. USA*, 2017, **114**, E3188-E3194.
18. P. J. Rayner, P. Norcott, K. M. Appleby, W. Iali, R. O. John, S. J. Hart, A. C. Whitwood and S. B. Duckett, *Nat. Commun.*, 2018, **9**, 4251.
19. S. S. Roy, P. J. Rayner, P. Norcott, G. G. R. Green and S. B. Duckett, *Phys. Chem. Chem. Phys.*, 2016, **18**, 24905-24911.
20. S. S. Roy, P. Norcott, P. J. Rayner, G. G. R. Green and S. B. Duckett, *Angew. Chem. Int. Ed.*, 2016, **55**, 15642-15645.
21. T. Theis, G. X. Ortiz, A. W. Logan, K. E. Claytor, Y. Feng, W. P. Huhn, V. Blum, S. J. Malcolmson, E. Y. Chekmenev, Q. Wang and W. Warren, *Sci. Adv.*, 2016, **2**, e1501438.
22. S. S. Roy, P. Norcott, P. J. Rayner, G. G. R. Green and S. B. Duckett, *Chem.- Eur. J.*, 2017, **23**, 10496-10500.
23. G. N. Zhang, J. F. P. Colell, T. Glachet, J. R. Lindale, V. Reboul, T. Theis and W. S. Warren, *Angew. Chem. Int. Ed.*, 2019, **58**, 11118-11124.
24. C. Bengs, L. Dagys, G. A. I. Moustafa, J. W. Whipham, M. Sabba, A. S. Kiryutin, K. L. Ivanov and M. H. Levitt, *J. Chem. Phys.*, 2021, **155**, 124311.